

Université de Liège  
Faculté des Sciences  
Département de Géologie  
Laboratoire de Minéralogie



# The Crystal Chemistry of Olivine-type Phosphates

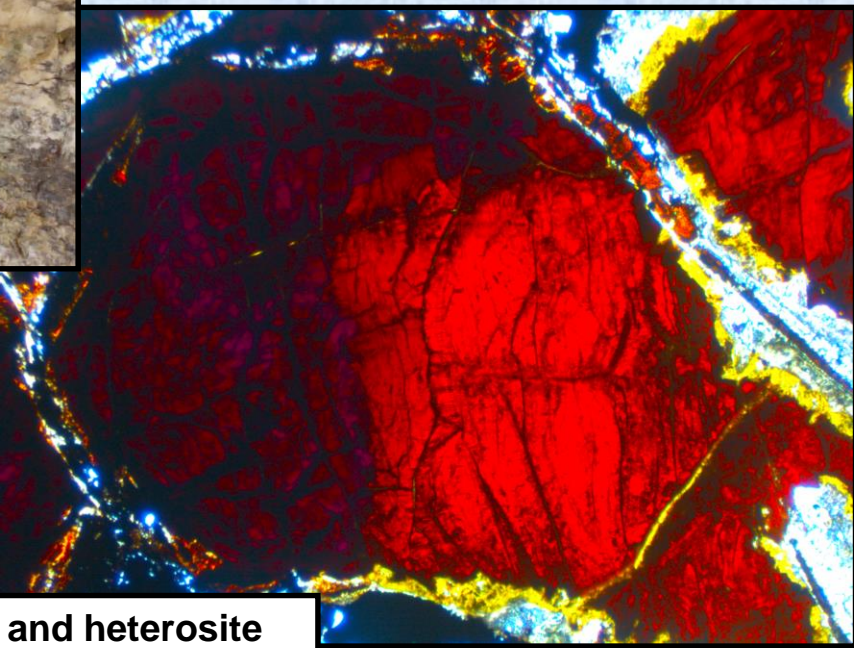
F. Hatert, L. Ottolini, F. Fontan, P. Keller,  
E. Roda-Robles, A.-M. Fransolet

Mendoza, February 21<sup>st</sup>, 2011

# Occurrence: Granitic pegmatites

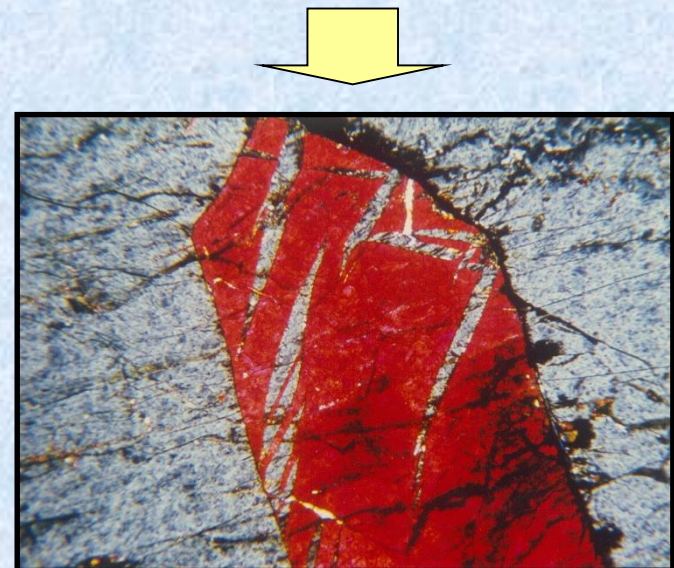
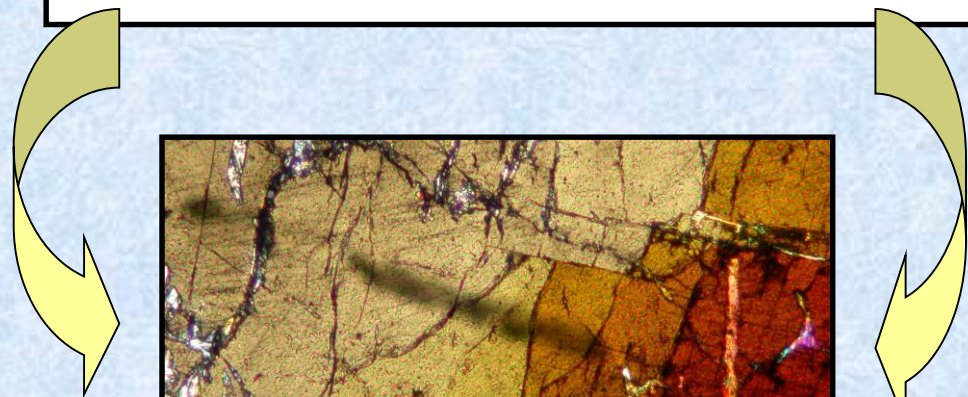
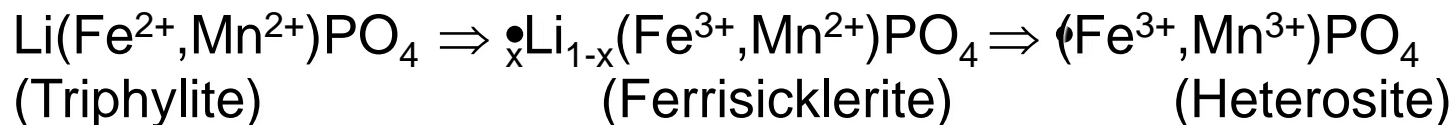


Ferrisicklerite and albite  
Sapucaia pegmatite, Brazil

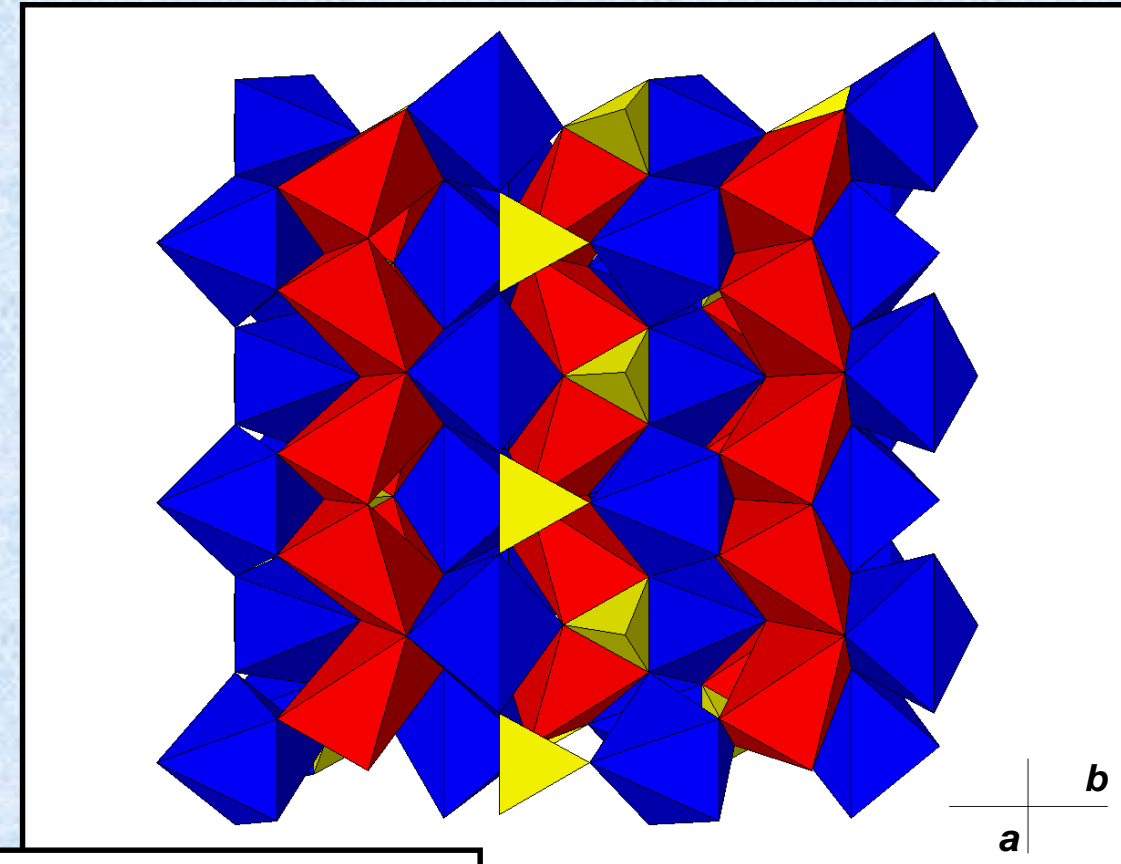


Ferrisicklerite and heterosite  
Boca Rica pegmatite, Brazil

# Oxidation of olivine-type phosphates: the « Quensel-Mason » sequence



# The triphylite structure



Red octahedra: M1  
Blue octahedra: M2

S.G. Pbnm

$a = 4.690$ ,  $b = 10.286$ ,  $c = 5.987 \text{ \AA}$

- M1: Li, []
- M2: Fe<sup>2+</sup>, Mn, Mg

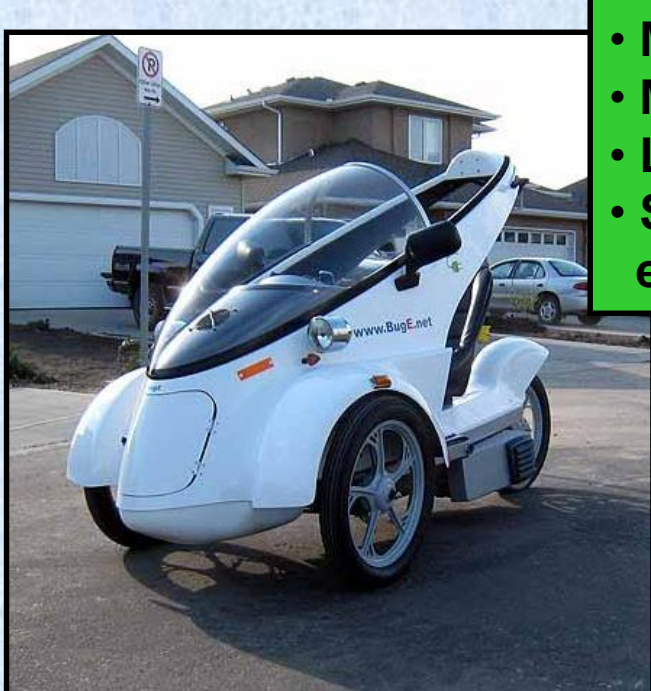
# LiFePO<sub>4</sub>-based batteries

nature

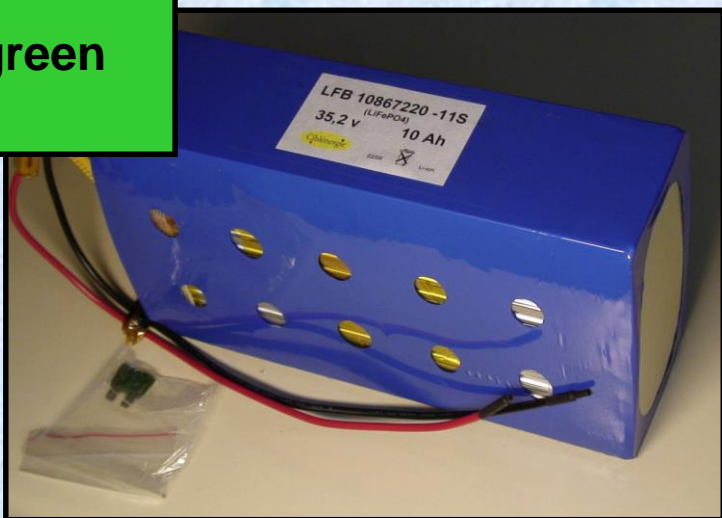
Vol 458 | 12 March 2009 | doi:10.1038/nature07853

## LETTERS

### Battery materials for ultrafast charging and discharging

Byoungwoo Kang<sup>1</sup> & Gerbrand Ceder<sup>1</sup>

- Cars
- Bicycles
- Motorbikes
- Mobile phones
- Laptops
- Storage of green energy



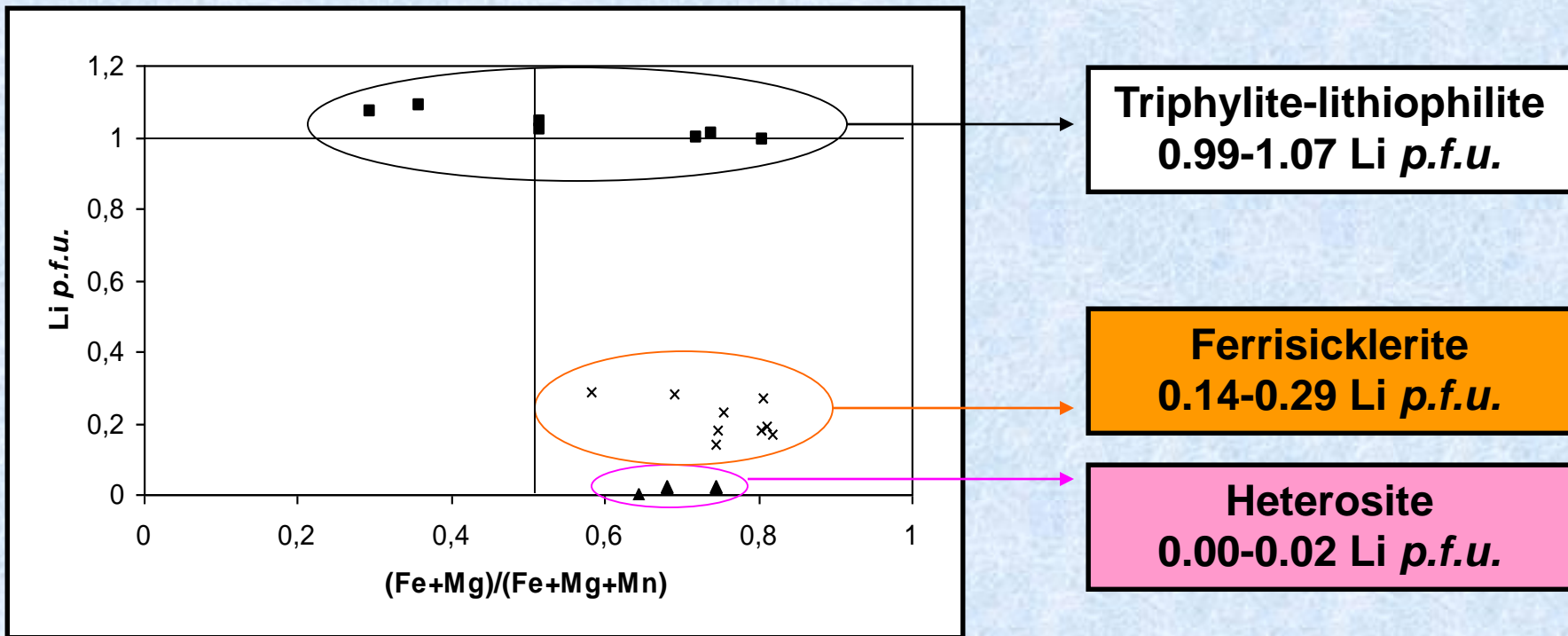
# Sample selection

Sample	Locality
PK-17	Hagendorf-Süd, Germany
PK-20	Engelbrechts Claim, Brandberg, Namibia
PK-1	McDonalds Claim, Brandberg, Namibia
PK-18	Strathmore tin mine, Namibia
PK-3	Ariakas, Usakos, Namibia
PK-15	Sandamap, Usakos, Namibia
K9-5-6 (5 zones)	Koktokay #3 pegmatite, Altai, China
AB-2-2	Cañada pegmatite, Spain
AB-X1-2-ME-3	Cañada pegmatite, Spain
AB-X1-2-TB-5	Cañada pegmatite, Spain

- Electron microprobe
- Ion probe (SIMS)
- Single-crystal structure refinements

Sample	Mineral	Composition
PK-17	Triphylite	$\text{Li}_{0.99}(\text{Fe}^{2+}_{0.73}\text{Fe}^{3+}_{0.05}\text{Mn}^{2+}_{0.19}\text{Mg}_{0.01})\text{PO}_4$
PK-20	Triphylite	$\text{Li}_{1.06}(\text{Fe}^{2+}_{0.65}\text{Mn}^{2+}_{0.34})\text{PO}_4$
PK-1	Ferrisicklerite	$\text{Li}_{0.18}(\text{Fe}^{3+}_{0.67}\text{Mn}^{2+}_{0.13}\text{Mn}^{3+}_{0.12}\text{Mg}_{0.07})\text{PO}_4$
PK-18	Ferrisicklerite	$\text{Li}_{0.18}(\text{Fe}^{3+}_{0.73}\text{Mn}^{2+}_{0.11}\text{Mn}^{3+}_{0.10}\text{Mg}_{0.06})\text{PO}_4$
PK-3	Heterosite	$(\text{Fe}^{3+}_{0.64}\text{Mn}^{2+}_{0.05}\text{Mn}^{3+}_{0.31}\text{Mg}_{0.01})\text{PO}_4$
PK-15	Heterosite	$\text{Li}_{0.02}(\text{Fe}^{3+}_{0.70}\text{Mn}^{3+}_{0.25}\text{Mg}_{0.03})\text{PO}_4$
AB-2-2	Ferrisicklerite	$\text{Li}_{0.17}(\text{Fe}^{3+}_{0.75}\text{Mn}^{2+}_{0.08}\text{Mn}^{3+}_{0.10}\text{Mg}_{0.06})\text{PO}_4$
AB-X1-2-ME-3	Ferrisicklerite	$\text{Li}_{0.19}(\text{Fe}^{3+}_{0.57}\text{Mn}^{3+}_{0.19}\text{Mg}_{0.24})\text{PO}_4$
AB-X1-2-TB-5	Ferrisicklerite	$\text{Li}_{0.23}(\text{Fe}^{3+}_{0.67}\text{Mn}^{2+}_{0.14}\text{Mn}^{3+}_{0.10}\text{Mg}_{0.07})\text{PO}_4$

# The Li content of natural olivine-type phosphates

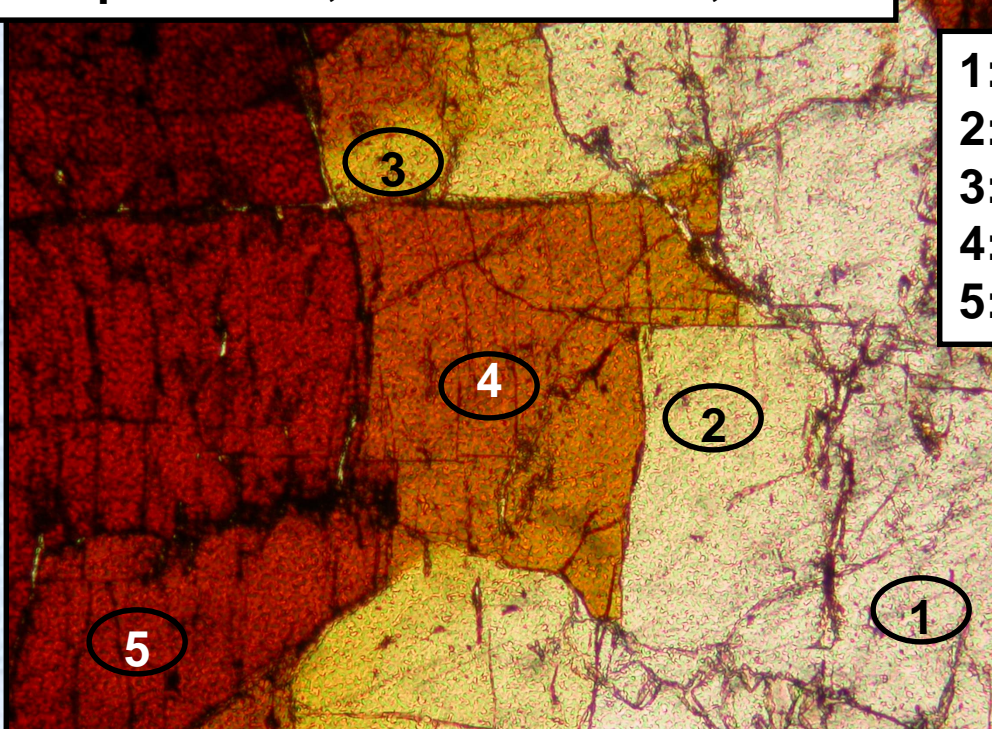


Heterosite may contain up to 0.21 wt. %  $\text{Li}_2\text{O}$ , and ferrisicklerite may show a low Li-content of 1.31 wt. %  $\text{Li}_2\text{O}$

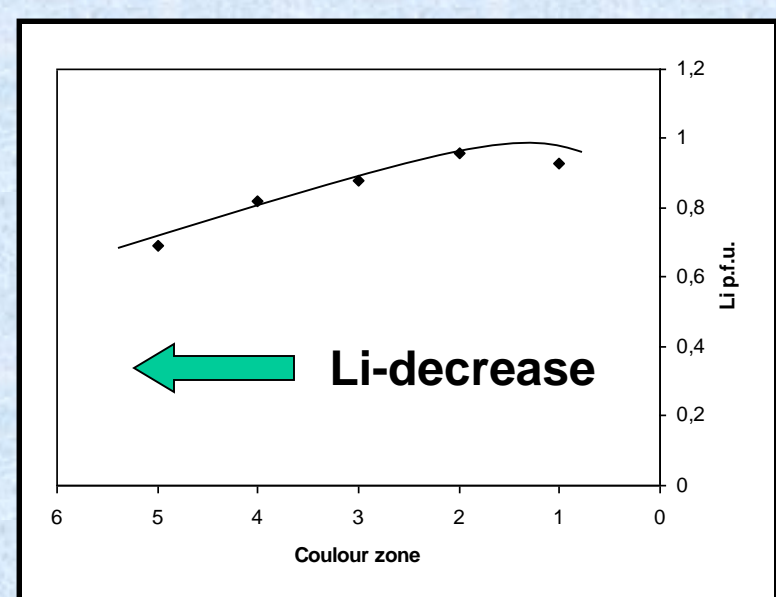
 Close Li-contents!

# The progressive transition from lithiophilite to sicklerite

Sample K9-5-6, Altaï Mountains, China



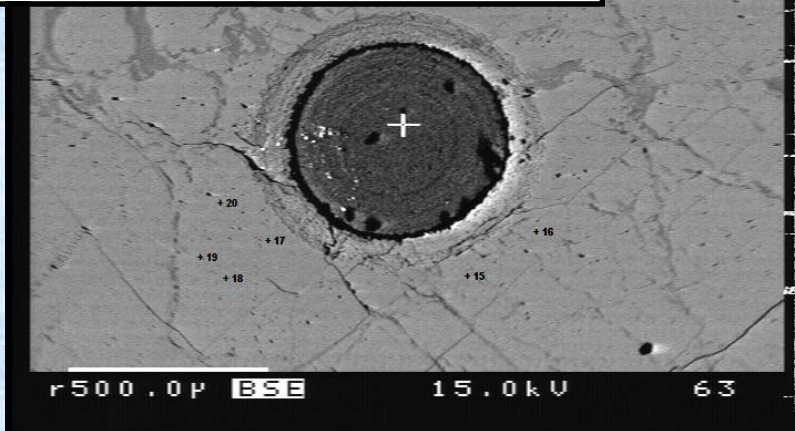
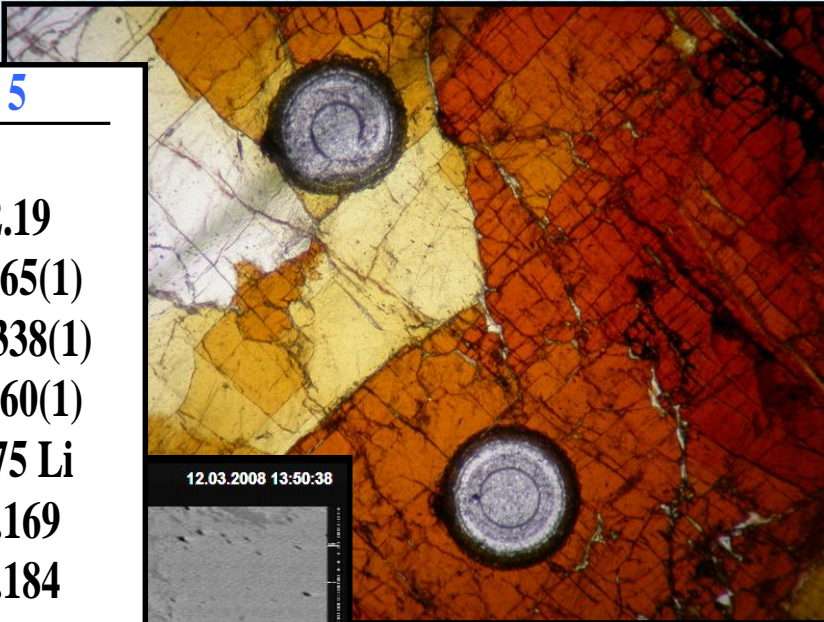
- 1:  $\text{Li}_{0.93}(\text{Fe}^{2+}_{0.03}\text{Fe}^{3+}_{0.13}\text{Mn}^{2+}_{0.80})(\text{PO}_4)$
- 2:  $\text{Li}_{0.96}(\text{Fe}^{2+}_{0.08}\text{Fe}^{3+}_{0.08}\text{Mn}^{2+}_{0.81})(\text{PO}_4)$
- 3:  $\text{Li}_{0.88}(\text{Fe}^{3+}_{0.16}\text{Mn}^{2+}_{0.80}\text{Mn}^{3+}_{0.01})(\text{PO}_4)$
- 4:  $\text{Li}_{0.82}(\text{Fe}^{3+}_{0.16}\text{Mn}^{2+}_{0.75}\text{Mn}^{3+}_{0.06})(\text{PO}_4)$
- 5:  $\text{Li}_{0.69}(\text{Fe}^{3+}_{0.16}\text{Mn}^{2+}_{0.62}\text{Mn}^{3+}_{0.19})(\text{PO}_4)$



- The transition from lithiophilite to sicklerite is progressive
- The change in colour is due to the presence of  $\text{Mn}^{3+}$

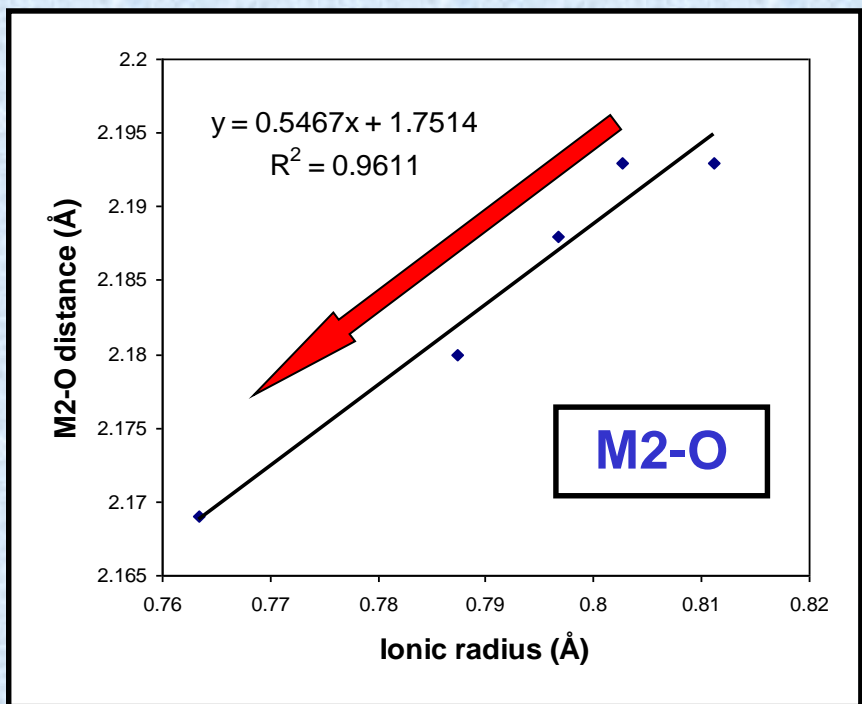
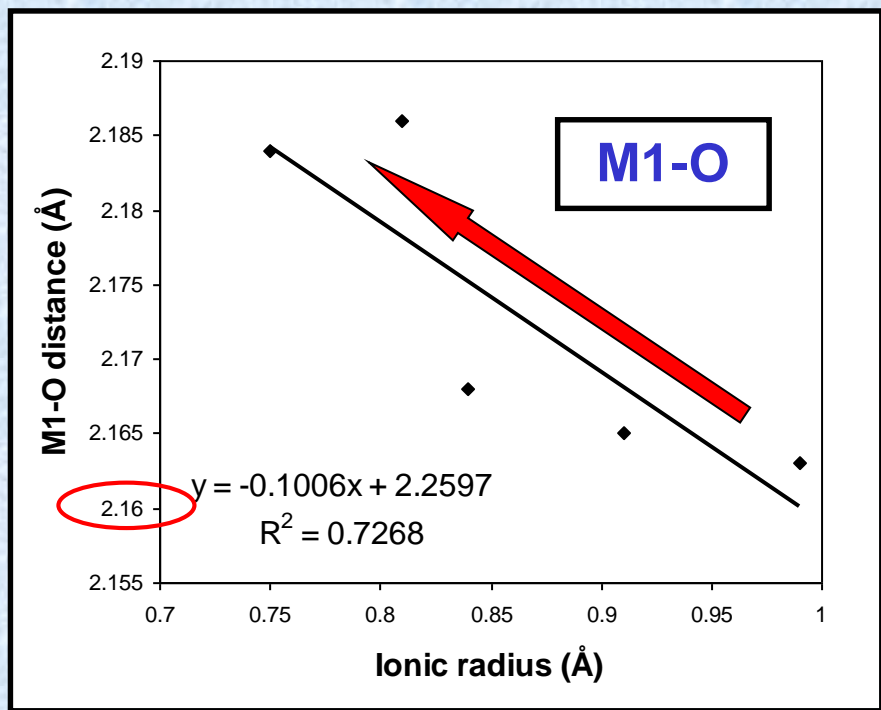
# A structural study of the lithiophilite-sicklerite series

	1	2	3	4	5
R <sub>1</sub> (%)	2.53	2.36	2.94	2.67	2.19
a (Å)	4.736(1)	4.734(1)	4.740(1)	4.767(1)	4.765(1)
b (Å)	10.432(2)	10.423(2)	10.415(1)	10.403(2)	10.338(1)
c (Å)	6.088(1)	6.094(1)	6.080(1)	6.072(1)	6.060(1)
M(2)	0.99 Li	0.91 Li	0.84 Li	0.81 Li	0.75 Li
M(1)-O	2.193	2.193	2.188	2.180	2.169
M(2)-O	2.163	2.165	2.168	2.186	2.184



- Micro-drilling
- Single-crystal structure refinements

# Variations of M-O bond lengths

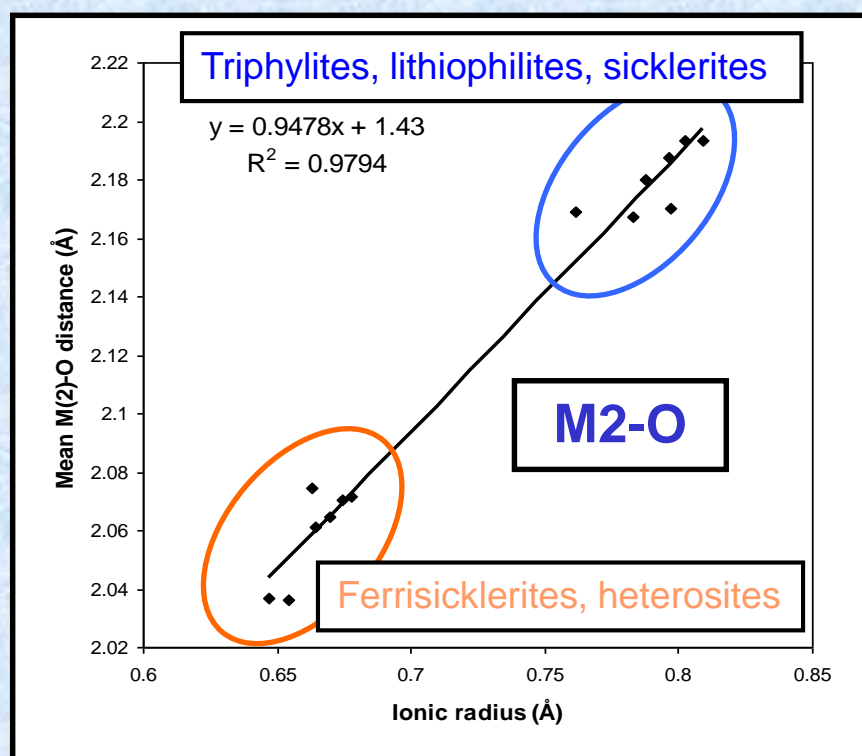
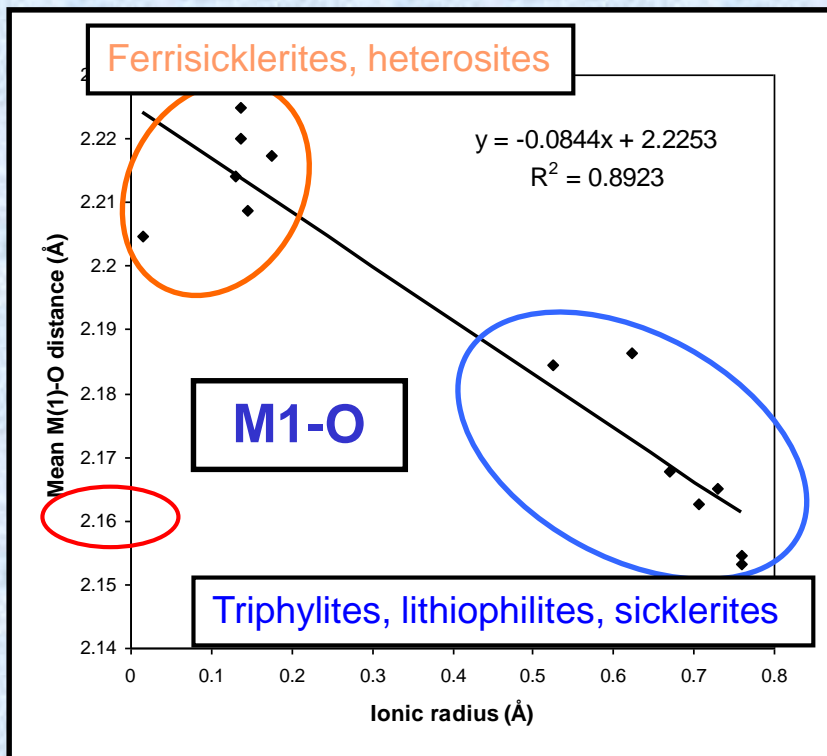


- Decrease of the M2-O bond lengths, due to the progressive oxidation of iron and manganese
- Increase of the M1-O bond lengths, due to leaching of lithium (decrease of bond valence sums correlated with the increasing number of vacancies)
- Correlation between M1-O and M2-O!

# Single-crystal structure refinements of natural olivine-type phosphates

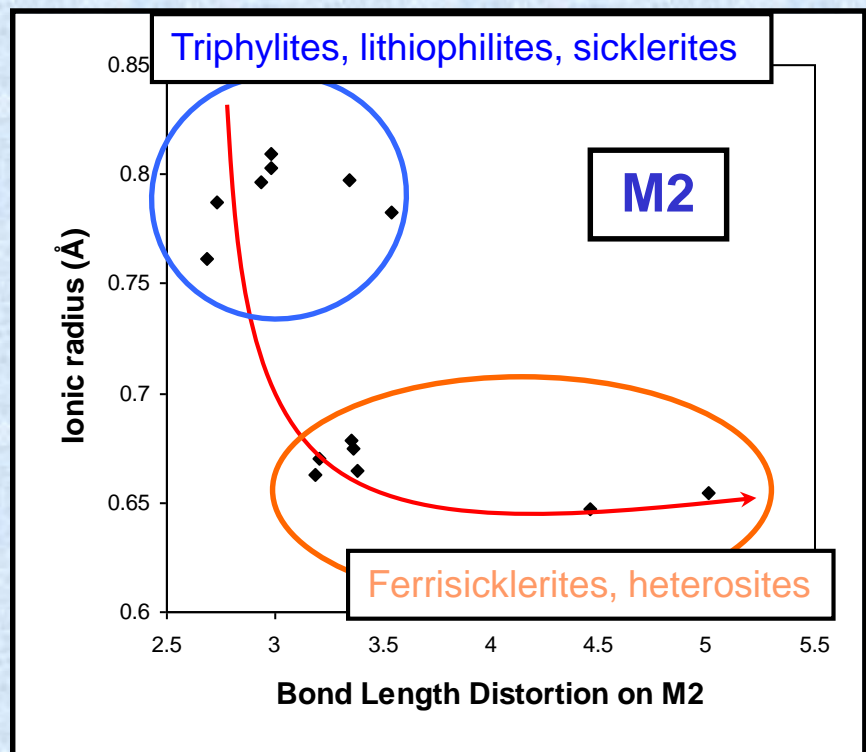
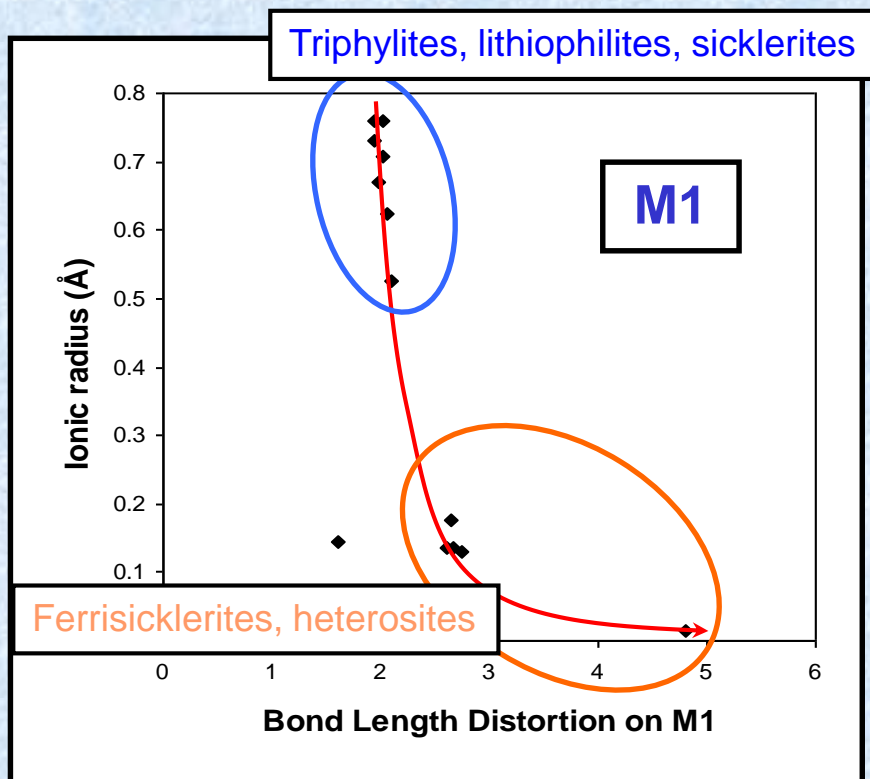
Sample	<i>a</i> (Å)	<i>b</i> (Å)	<i>c</i> (Å)	V (Å <sup>3</sup> )	R <sub>1</sub> (%)
PK-17	4.704(1)	10.365(1)	6.025(1)	293.7(1)	4.07
PK-20	4.711(1)	10.369(1)	6.038(7)	294.9(1)	3.56
PK-1	4.795(1)	9.979(2)	5.890(1)	281.8(1)	4.01
PK-18	4.795(2)	9.959(6)	5.892(3)	281.3(3)	4.92
PK-3	4.776(3)	9.732(3)	5.826(3)	270.8(2)	6.32
PK-15	4.777(2)	9.776(3)	5.817(2)	271.7(2)	5.76
AB-2-2	4.787(2)	9.954(3)	5.875(2)	280.0(2)	5.87
AB-X1-2-ME-3	4.776(3)	10.035(3)	5.883(3)	282.0(3)	8.24
AB-X1-2-TB-5	4.797(3)	9.978(5)	5.881(3)	281.5(3)	6.92

# Variations of M-O bond lengths



- Decrease of the M2-O due to the progressive oxidation of iron and manganese
- Increase of the M1-O due to leaching of lithium

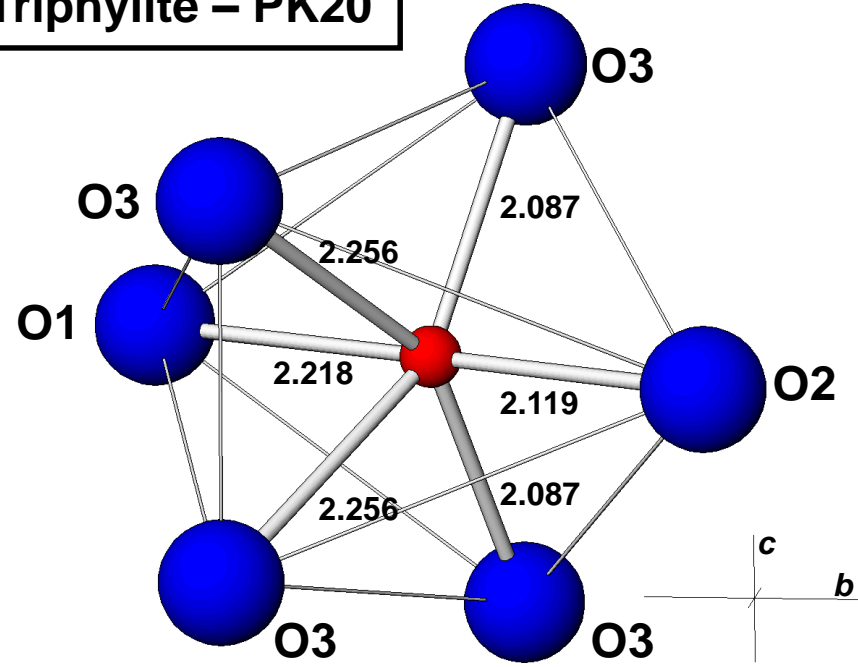
# Distortion coefficients



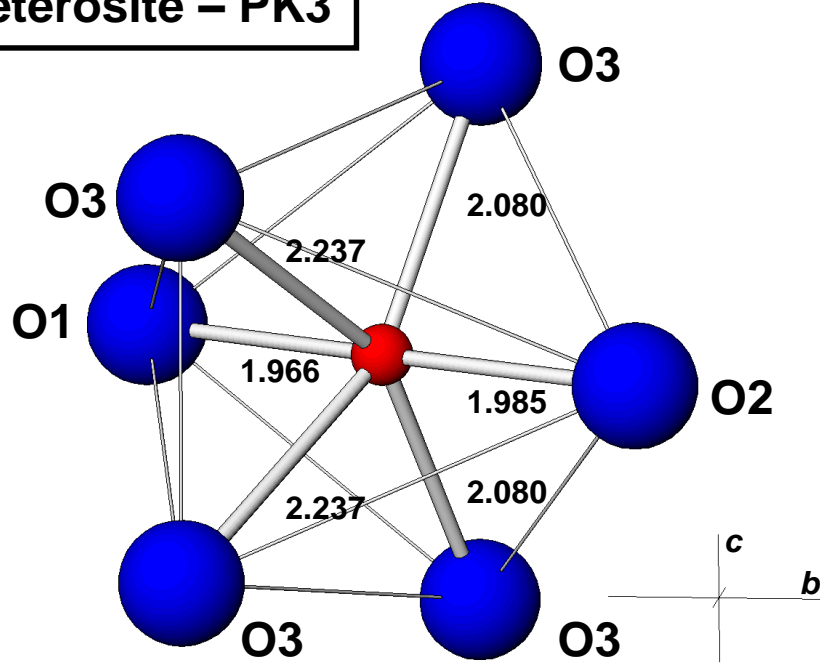
Increase of the M1 and M2 bond length distortion coefficients for the oxidized compositions (ferrisicklerites, heterosites)

# Topology of the M2 site

Triphylite – PK20

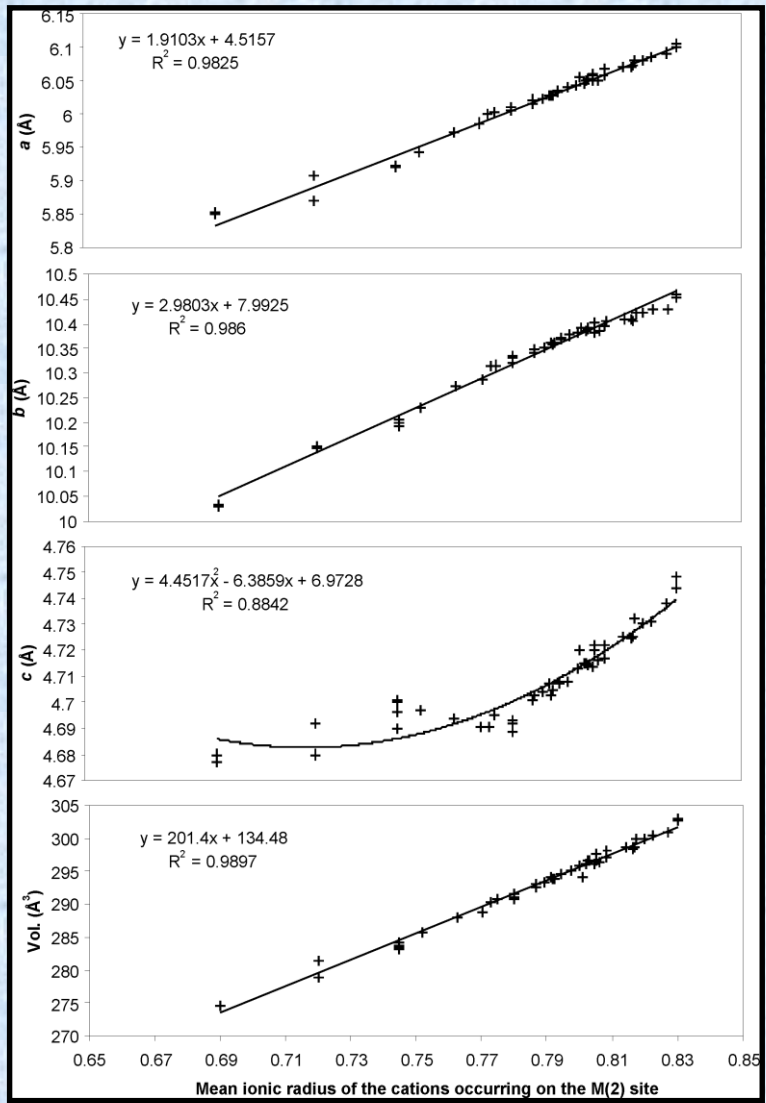


Heterosite – PK3

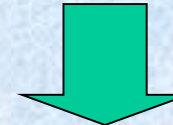


Jahn-Teller distortion, due to the presence of Mn<sup>3+</sup> in heterosite

# Variations of unit-cell parameters



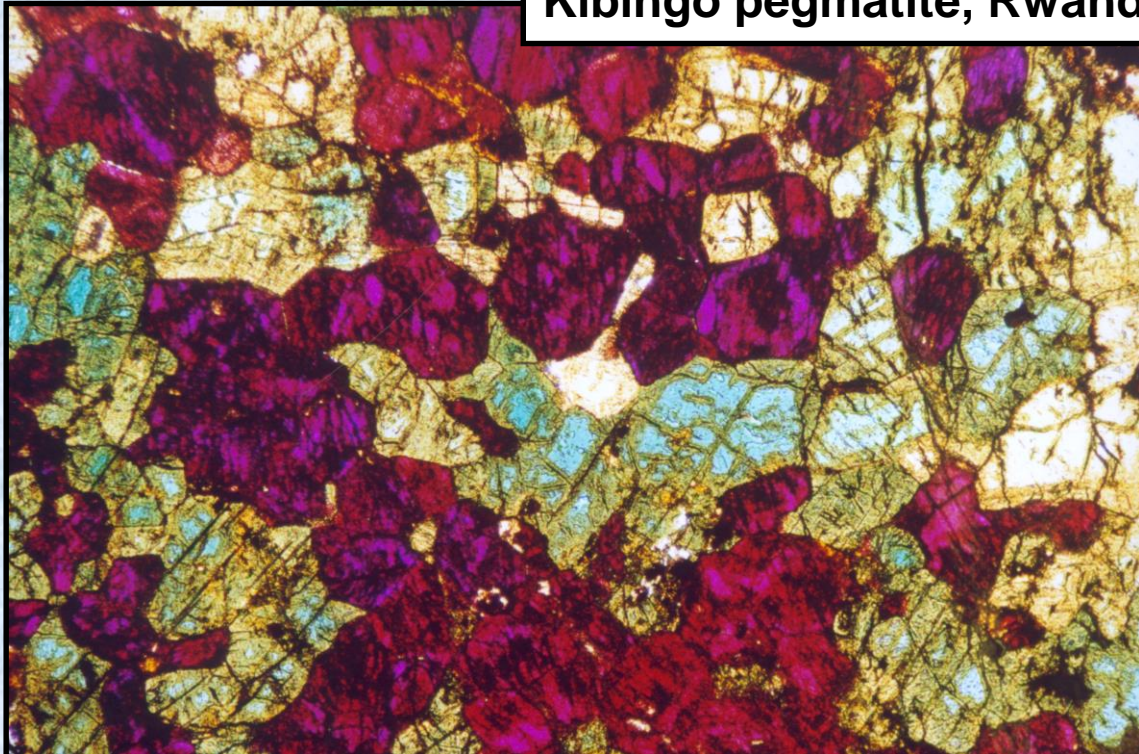
Good correlations



Accurate estimation of the Fe/Mn ratio of natural members of the triphylite-lithiophilite series, when the Mg content is lower than 0.016 a.p.f.u. (accuracy +/- 7 %)

# Experimental investigations: the alluaudite + triphylite assemblage

Kibingo pegmatite, Rwanda

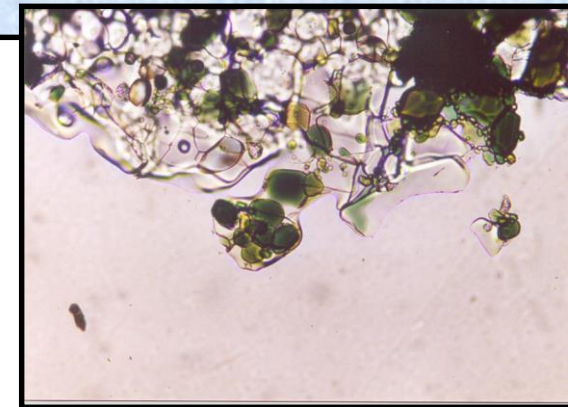
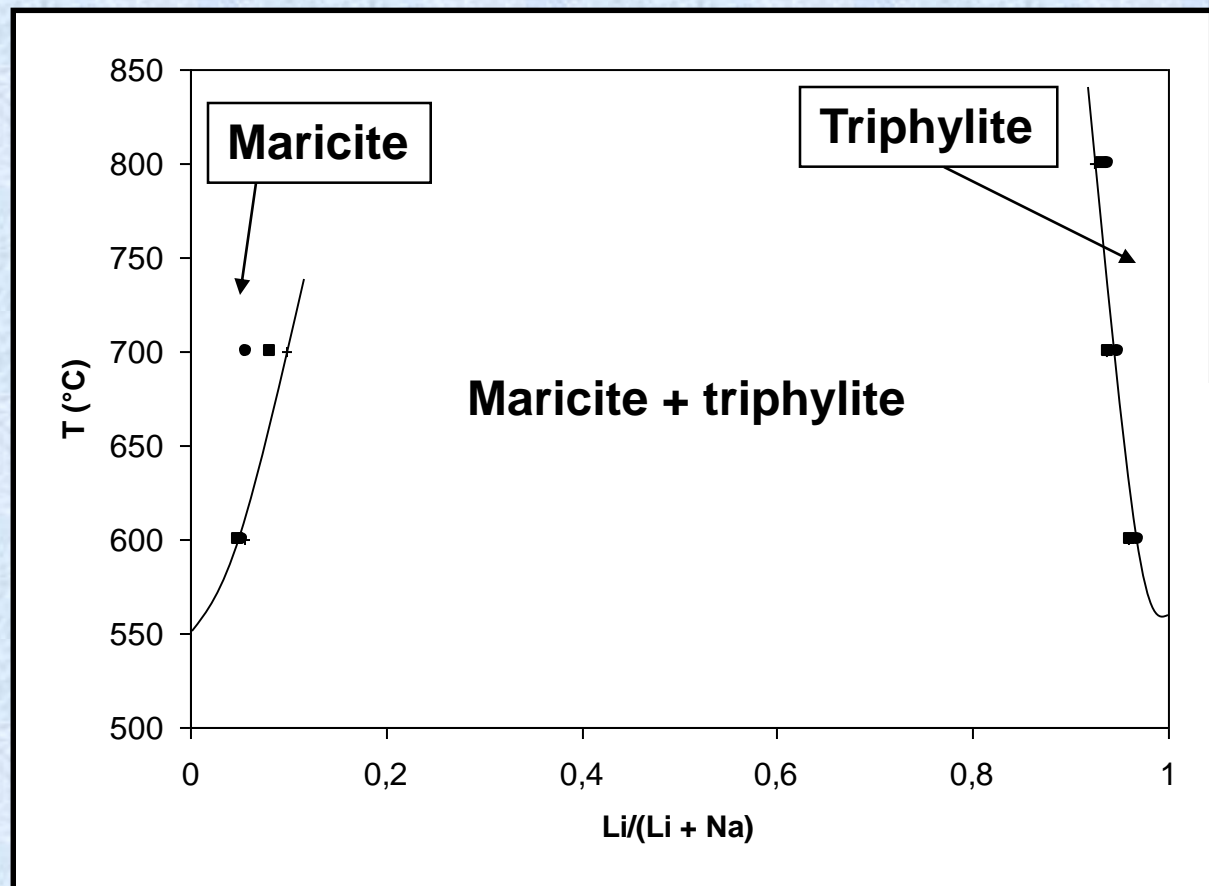


## Hydrothermal synthesis

T = 400-800 °C, P = 1 kbar



# Presence of Na in synthetic triphylite

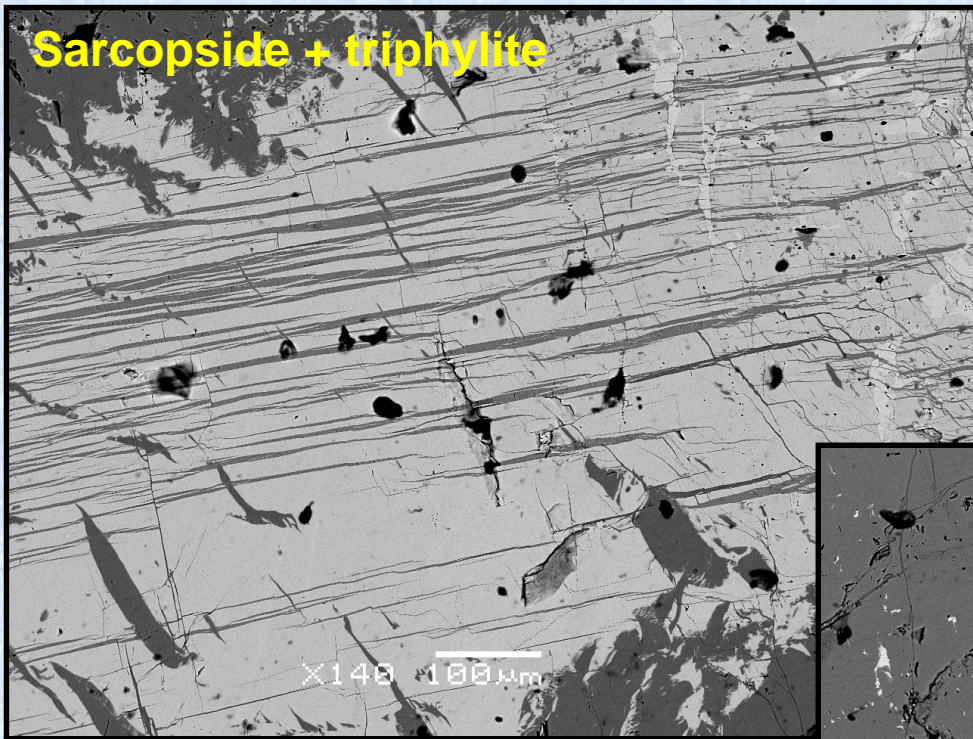


- In triphylite, Na can reach 0.08 a.p.u.f. at 800°C
- In maricite, Li can reach 0.10 a.p.u.f. at 700°C

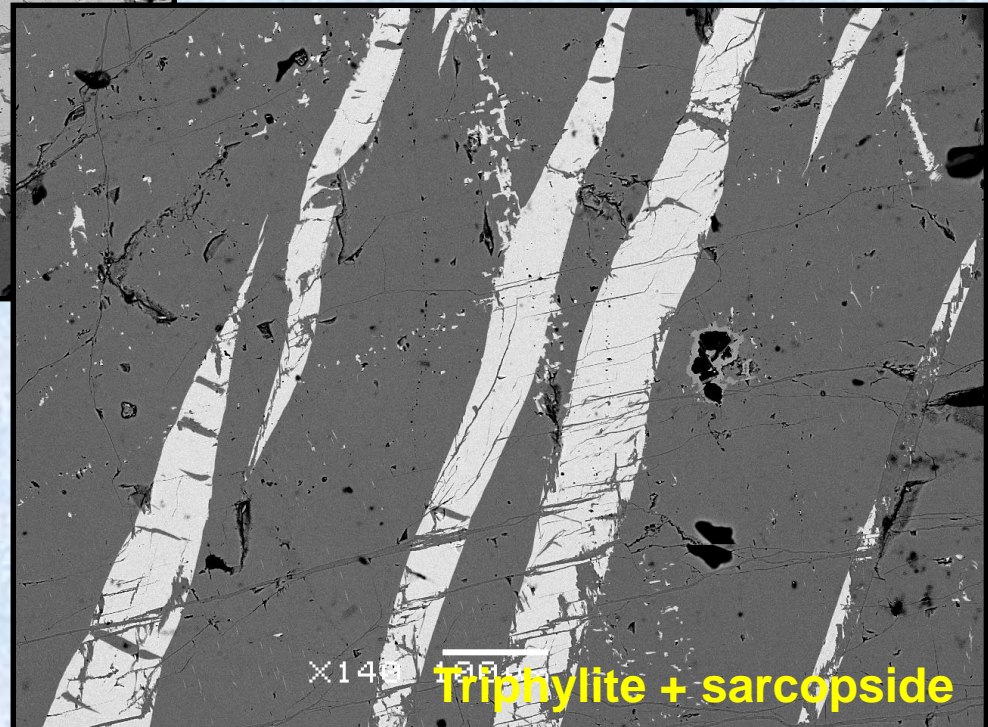


**Na already observed in natrophilite,  $\text{NaMnPO}_4$ !**

# The triphylite + sarcopside assemblage



Cañada pegmatite,  
Spain



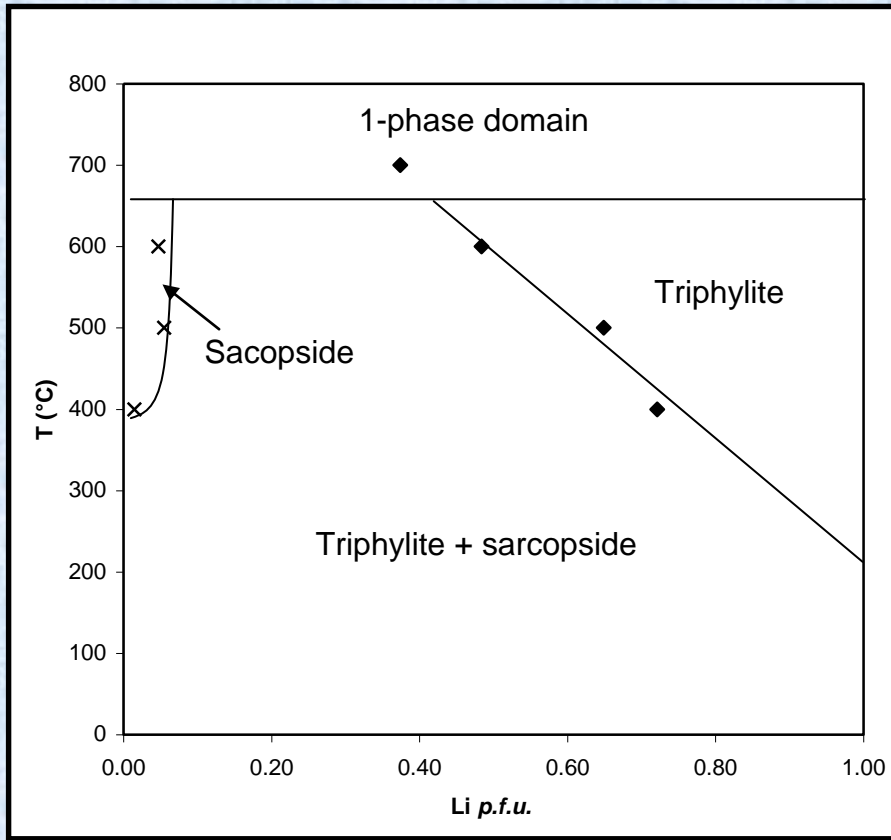
Lamellar textures



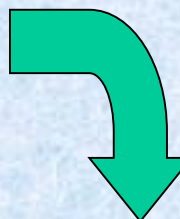
EXSOLUTIONS!!

Sarcopside ( $\text{Fe},\text{Mn}$ )<sub>3</sub>(PO<sub>4</sub>)<sub>2</sub>

# Stability of the triphylite + sarcopside assemblage



- Decrease of the Li-content of triphylite, from 0.72 a.p.f.u. at 400°C, to 0.48 a.p.f.u. at 600°C
- 1-phase domain above 650°C



- The Li-content of triphylite decreases with the temperature
- The Fe-content of triphylite increases with the temperature

# Conclusions

- Natural and synthetic olivine-type phosphates were investigated by single-crystal X-ray diffraction, electron-microprobe, and ion probe (SIMS) techniques.
- The Li contents of ferrisicklerites and heterosites are very close to each other, and a progressive oxidation from lithiophilite to sicklerite is observed.
- The oxidation from triphylites to heterosites provokes a decrease of the M2-O bond lengths due to the oxidation of Fe and Mn, as well as an increase of the M1-O bond lengths due to the leaching of Li.
- A Jahn-Teller distortion of the M2 site is observed in heterosites, due to the presence of Mn<sup>3+</sup>.
- Hydrothermal experiments have shown that significant amounts of Na may occur on the M1 site, and that Li may be replaced by Fe and vacancies according to the substitution mechanism  $2\text{Li}^+ = \text{Fe}^{2+} + []$ .